# New isomers and medium-spin structure of the $^{95}$Y nucleus

W. Urban,[1,2] K. Sieja,[3] G. S. Simpson,[1,4] H. Faust,[1] T. Rząca-Urban,[2] A. Złomaniec,[2] M. Łukasiewicz,[2]
A. G. Smith,[5] J. L. Durell,[5] J. F. Smith,[5] B. J. Varley,[5] F. Nowacki,[6] and I. Ahmad[7]

[1]*Institut Laue-Langevin, 6 rue J. Horowitz, F-38042 Grenoble, France*
[2]*Faculty of Physics, University of Warsaw, ul. Hoża 69, PL-00-681 Warsaw, Poland*
[3]*Gesellschaft für Schwerionenforschung, Planckstrasse 1, D-64291 Darmstadt, Germany and Institut für Kernphysik, Technische Universität Darmstadt, D-64289 Darmstadt, Germany*
[4]*Laboratoire de Physique Subatomique et de Cosmologie, IN2P3-CNRS/Université J. Fourier, F-38026 Grenoble Cedex, France*
[5]*Department of Physics and Astronomy, The University of Manchester, M13 9PL Manchester, United Kingdom*
[6]*Institute Pluridisciplinaire Hubert Curien, 23 rue du Loess, F-67037 Strasbourg Cedex, France*
[7]*Argonne National Laboratory, Argonne, Illinois 60439, USA*

(Received 20 December 2008; published 6 April 2009)

Excited states in $^{95}$Y, populated following the spontaneous fission of $^{248}$Cm and $^{252}$Cf and following fission of $^{235}$U induced by thermal neutrons, were studied by means of $\gamma$ spectroscopy using the EUROGAM2 and GAMMASPHERE multidetector Ge arrays and the LOHENGRIN fission-fragment separator, respectively. We have found a new $(17/2^-)$ isomer in $^{95}$Y at 3142.2 keV with a half-life of $T_{1/2} = 14.9(5)$ ns. Another isomer was identified in $^{95}$Y at 5022.1 keV and it was assigned a spin-parity $(27/2^-)$. For this isomer a half-life of $T_{1/2} = 65(4)$ ns was determined and four decay branches were found, including an $E3$ decay. A new $E3$ decay branch was also found for the known, 1087.5-keV isomer in $^{95}$Y, for which we measured a half-life of 51.2(9) $\mu$s. The $B(E3)$ and $B(E1)$ transition rates, of 2.0 and $3.8 \times 10^{-7}$ W.u., respectively, observed in $^{95}$Y are significantly lower than in the neighboring $^{96}$Zr core, suggesting that octupole correlations in this region are mainly due to the coupling of proton $\Delta j = 3$ orbitals. Shell-model calculations indicate that the $(27/2^-)$ isomer in $^{95}$Y corresponds to the $\pi g_{9/2}\nu(g_{7/2}h_{11/2})$ maximally aligned configuration and that all three isomers in $^{95}$Y decay, primarily, by $M2$ transitions between proton $g_{9/2}$ and $f_{5/2}$ orbitals.

DOI: 10.1103/PhysRevC.79.044304 PACS number(s): 21.10.Tg, 23.20.Lv, 25.85.Ec, 27.60.+j

## I. INTRODUCTION

It has been shown in recent years that the onset of deformation in the $A \sim 100$ region is related to the population of the neutron intruder orbital $\nu h_{11/2}$ [1–3]. It is therefore of interest to study in detail the properties of the $\nu h_{11/2}$ shell, especially around the neutron number $N = 59$ where the deformation emerges. Although the presence of the $\nu h_{11/2}$ orbital in nuclei with $N > 58$, where the deformation onset is clearly in progress, is well documented, the information about this orbital in nuclei with $N \leqslant 58$ is still limited. This work is a continuation of our search [4] for the characteristic $\nu(g_{7/2}h_{11/2})_{9^-}$, two-neutron excitations in nuclei with $N \leqslant 58$, which should help in finding the position of the spherical $\nu h_{11/2}$ orbital.

It should be noted that although the mean-field approach, described in Refs. [1,2], provides a solution where the deformed minimum in the potential is clearly connected with the population of the $\nu h_{11/2}$ intruder, it does not draw any simple description of forces causing the sudden shape change observed around neutron number $N = 59$. A phenomenological picture proposed recently [5], which involves the so-called, extruder orbital $\nu_{9/2}[404]$, offers a mechanism producing strongly deformed configurations, indeed observed at neutron number $N = 59$ [6]. However, it remains to be checked whether this mechanism is present (or if it can be introduced) in the mean-field calculations. In contrast, a very specific description of a shape-driving mechanism was proposed in the past, invoking the $\pi g_{9/2}$-$\nu g_{7/2}$ proton-neutron residual interaction, the so-called spin-orbit partners mechanism [7]. However attractive, this mechanism does not involve $h_{11/2}$ neutrons, which is inconsistent with the experimental evidence of their presence near the Fermi level around $N = 59$ [3,8]. As discussed in our recent work [4], the proton-neutron interaction derived from the tensor force [9] should be vital in shaping the shell structure of nuclei and it is important to verify its role as well as to check the role of $h_{11/2}$ neutrons in the sudden shape change observed in the $A \sim 100$ neutron-rich nuclei. A theoretical work in this direction is in progress [10].

The experimental observation of the $\nu h_{11/2}$ and/or $\nu(g_{7/2}h_{11/2})_{9^-}$ negative-parity excitations in this region becomes even more important in light of recent detailed studies of spherical Zr isotopes [11]. The authors concluded there that negative-parity levels in $^{92-96}$Zr are due to proton excitations from the $\pi p_{1/2}, \pi p_{3/2}$, or $\pi f_{5/2}$ orbitals up to the $\pi g_{9/2}$ orbital. This proposition was based on comparing experimental data with shell-model calculations. However, in the calculations of Ref. [11] the single-particle space was truncated because of computational limitations. The crucial $h_{11/2}$ neutron orbital was not included in the model space. Experimental identification of $\nu(g_{7/2}h_{11/2})_{9^-}$ excitations in nuclei from this region may help clear up the situation.

In the Zr isotopes, the $\nu(g_{7/2}h_{11/2})_{9^-}$ neutron excitation may be located close to another $9^-$ excitation, corresponding to the $2^+ \otimes \pi(f_{5/2}g_{9/2})_{7^-}$ proton coupling. This could make the differentiation between proton- and neutron-based, negative-parity excitations difficult. It may be easier to search for the $\nu(g_{7/2}h_{11/2})_{9^-}$ excitation in yttrium isotopes, where the proton-based, negative-parity levels, involving three-proton

 

excitations, are expected at higher excitation energies than the negative-parity levels, corresponding to one proton coupled to the $\nu(g_{7/2}h_{11/2})_{9^-}$ neutron configuration.

Of two yttrium isotopes with $N < 58$,[95,96]Y, where the $h_{11/2}$ neutron orbital should already be populated, $^{95}$Y is a better candidate for medium-spin studies. In this nucleus a $T_{1/2} = 56.2\ \mu s$ isomer with spin $9/2^+$ was reported at 1087.5 keV [12]. No higher lying levels were known in $^{95}$Y. One expects, though, that levels above the isomer in $^{95}$Y should be sufficiently populated to allow such studies because the average spin populated in fission is higher than the spin of this isomer. The situation is less favorable for $^{96}$Y where the $T_{1/2} =$ 9 s isomer at 1140(30) keV, interpreted as a $(\pi g_{9/2}\nu g_{7/2})_{8^+}$ configuration, has a rather high spin, $I^\pi = 8^+$ [13,14]. In $^{96}$Y one may still find the $(\pi g_{9/2}\nu h_{11/2})_{10^-}$ excitation about 1 MeV above the isomer. However, higher spin excitations, as for instance the $[(\pi g_{9/2}\nu g_{7/2})_{8^+} \otimes \nu(h^2_{11/2})_{10^+}]_{18^+}$ configuration, will require breaking of a neutron pair plus about 2 MeV of excitation energy to promote neutrons to the $\nu h_{11/2}$ level. Therefore, they are expected at much higher energies, where the population in fission is weak. Despite these odds a high-spin state was proposed in $^{96}$Y [15] located 3932 keV above the $0^-$ ground state. Its observation was helped by the isomeric character of this state, for which a half-life of $T_{1/2} = 165(42)$ ns was reported [15]. The spin of this isomer, as estimated from the structure of the isomeric cascade, should be around $10\hbar$. This is rather inconsistent with what has been said above about $^{96}$Y and raises questions about the nature of this isomer, which should rather promptly decay to the $8^+$ level.

In this work we report on a study of medium-spin levels in the $^{95}$Y nucleus, investigated with the primary goal to search for excitations involving the $\nu(g_{7/2}h_{11/2})_{9^-}$ neutron configuration. Additional motivation for our study was to answer questions concerning the proposed isomeric cascade in $^{96}$Y. Section II of this work describes the experiments, the data analysis, and the results of our measurements. In Sec. III the experimental data are compared to the shell-model calculations and single-particle configurations are proposed for excited levels. The work is summarized in Sec. IV.

## II. EXPERIMENTAL STUDIES OF $^{95}$Y

Three experiments were preformed to study $^{95}$Y, the measurement of prompt $\gamma$ rays following spontaneous fission of $^{248}$Cm using the EUROGAM 2 array, the measurement of prompt $\gamma$ rays following spontaneous fission of $^{252}$Cf using the GAMMASPHERE array, and the measurement of delayed $\gamma$ radiation following neutron-induced fission of $^{235}$U, performed with the LOHENGRIN mass spectrometer. In the following we describe these experiments and their respective results.

### A. Measurement of prompt $\gamma$ rays following spontaneous fission of $^{248}$Cm

In $^{95}$Y one observes four states corresponding to proton orbitals available at the Fermi level. These are the $\pi p_{1/2}$ ground state, the $\pi p_{3/2}$ and $\pi f_{5/2}$ excited states at 685.7 and 826.8 keV, respectively, and the $9/2^+$, isomer at 1087.5 keV, reported previously with $T_{1/2} = 56.2(1.5)\ \mu s$, corresponding to the $\pi g_{9/2}$ configuration [16–20]. The isomeric level decays to the 826.8-keV level by the 260.7-keV, single-particle $M2$ transition with the rate of 0.021 W.u. [12]. The presence of the long-lived (56-$\mu s$) isomer obstructs $\gamma$-coincidence studies of higher spin excitations in $^{95}$Y. However, they can be identified because fission fragments are produced in pairs. Prompt $\gamma$ rays de-exciting levels above the 56-$\mu s$ isomer in $^{95}$Y are expected to be in coincidence with prompt $\gamma$ rays de-exciting levels in $^{147,149}$La nuclei, the most abundant fission-fragment partners to $^{95}$Y, produced in spontaneous fission of $^{248}$Cm.

We have searched for medium-spin levels in $^{95}$Y above the 56-$\mu$s isomer using triple-$\gamma$ coincidences between prompt $\gamma$ rays from fission fragments produced in spontaneous fission of $^{248}$Cm, measured with the EUROGAM 2 [21] array of Anti-Compton Spectrometers (ACS). (For additional details on the experiment and data analysis techniques see Refs. [22–24].) In spontaneous fission of $^{248}$Cm about 3.5 neutrons (on average) and no protons are emitted from the primary fission fragments, leading to the secondary fission fragments, which then de-excite by emitting $\gamma$ rays. Each fission event produces a pair of secondary fragments, which have in total 96 protons and, on average, about 245 neutrons. Prompt $\gamma$ rays from both fragments of a given pair are emitted at the same time (i.e., are in time coincidence). This allows us to perform searches for unknown $\gamma$ cascades in a nucleus if the fission partner has known decays.

The most abundant fission partner to $^{95}$Y, corresponding to the four-neutron evaporation channel, is $^{149}$La. In the spectra double gated on lines in $^{149}$La [25], we observed two new lines at 969.1 and 1085.8 keV, which do not belong to $^{149}$La. The same two lines are also seen in a spectrum doubly gated on lines in $^{147}$La [26]. This indicates that the 969.1- and 1085.8-keV lines belong to an yttrium isotope. A spectrum doubly gated on the 317-keV line from $^{149}$La and the 969.1-keV line, shown in Fig. 1(a), contains the 199.3- and 418.2-keV lines of $^{149}$La, the 1085.8-keV line, and further lines at 171.8, 461.5, and 564.1 keV.

The 171.8-, 461.5-, 564.1-, 969.1-, and 1085.8-keV lines were observed previously and assigned to $^{96}$Y in a measurement of delayed $\gamma$ transitions populated in heavy-ion-induced fission [15], where a 682-keV transition was also reported. The assignment of the discussed cascade to $^{96}$Y in

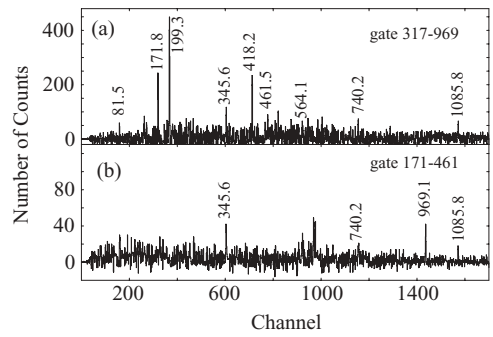


FIG. 1. Coincidence spectra gated on $\gamma$ lines in $^{149}$La and $^{95}$Y obtained in this work from fission of $^{248}$Cm. Energies of transitions and gates are labeled in keV.

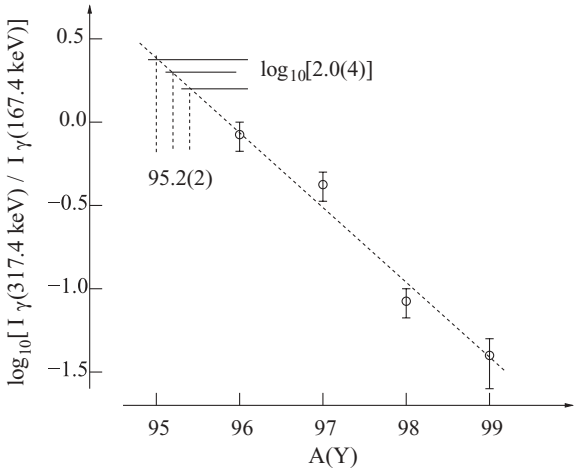


FIG. 2. Mass correlation diagram for yttrium and lanthanum isotopes produced in fission of $^{248}$Cm. See text for further explanation.

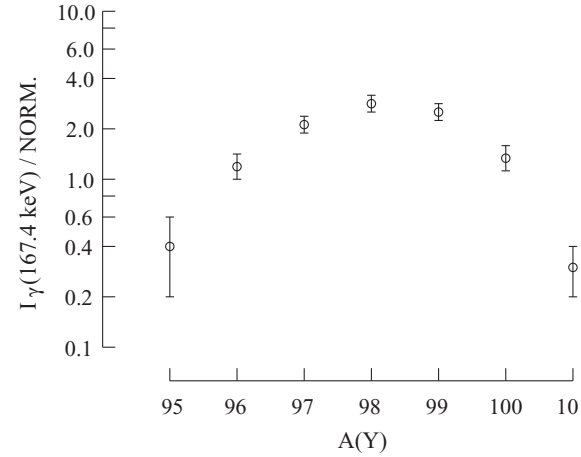


FIG. 3. Rates of yttrium isotopes in coincidence with the $^{147}$La nucleus as produced in the fission of $^{248}$Cm. See text for further explanation.

Ref. [15] was based on a measurement using the SAPhIR fission-fragment detector, allowing mass determination with accuracy of approximately 1 mass unit. We have checked this identification using the mass correlation technique for the complementary fission fragments, as proposed in Ref. [8], and have applied this technique successfully since then in many cases [25,27,28]. In Fig. 2 we show the mass correlation plot, where on a $\log_{10}$ scale the ratio $R$ of the intensity of the 317.4-keV transition in $^{149}$La to the intensity of the 167.4-keV transition in $^{147}$La, as observed in spectra doubly gated on known yrast cascades in various Y isotopes, is drawn. Because of the correlation between the masses of a given lanthanum isotope and its Y fission-fragment partners [29], such a ratio is a smooth function of mass $A$ of yttrium isotopes. The dashed line represents a linear fit to the $\log_{10}(R)$ values obtained for yrast cascades in $^{99}$Y, $^{98}$Y, $^{97}$Y, and $^{96}$Y (open circles). The ratio obtained for the cascade studied in this work is $R = 2.0(4)$ and the corresponding $\log_{10}(R)$ value is marked in Fig. 2. Intersection of this value with the straight-line fit gives a mass value of $A = 95.2(2)$, which uniquely correlates this cascade with $^{95}$Y. We propose that this cascade feeds the 1087.5-keV isomer in $^{95}$Y. An alternative placement of the cascade, directly on the ground state, is less likely because then the hypothetical $5/2^-$ level at 1085.8 keV would be rather nonyrast. Moreover, there should be a $3/2^-$ level at 740.2 keV, populated in the decay of the 1087.5-keV isomer, which is not observed.

In addition to this mass correlation we show in Fig. 3 coincidence rates of various yttrium isotopes with $^{147}$La nucleus, as produced in fission of $^{248}$Cm. The rates were calculated as the relative intensity of the 167.4-keV line in $^{147}$La observed in a spectrum double gated on the strongest lines in a complementary Y isotope. This intensity is then normalized by (i) the $\gamma$-detection efficiency at different gate energies, (ii) the gate width, and, (iii) the relative intensity of the gated cascade in this yttrium isotope. Despite the approximate character of this definition, the rates in Fig. 3 display a variation [as function of the yttrium mass, $A$(Y)], which is regular enough to draw conclusions. The rate corresponding to the 969.1- to 1085.8-keV cascade follows the smooth trend when placed at $A = 95$. This is consistent with the identification shown in Fig. 2.

The 172-, 461-, 563-, 682-, 968-, and 1086-keV transitions reported in Ref. [15] were arranged in a cascade de-exciting a high-spin isomer in the following order: 1086, 968, 461, 172, 682, and 563 keV, when going from the bottom of the cascade up to the isomer. This order is not consistent with intensities of $\gamma$ lines seen in our spectra, which are shown in the second column of Table I. For instance, the intensity of the 564.1-keV line in Fig. 1(a) is clearly higher than that

TABLE I. Intensities of $\gamma$ transitions in the $^{95}$Y nucleus, populated in the spontaneous fission of $^{248}$Cm, in the spontaneous fission of $^{252}$Cf, and in thermal-neutron-induced fission of $^{235}$U, as observed in the present work.

| $E_\gamma$ (keV) | $I_\gamma$ (rel.) $^{248}$Cm | $I_\gamma$ (rel.) $^{252}$Cf | $I_\gamma$ (rel.) $^{235}$U + $n_{th}$ |
|---|---|---|---|
| 101.2 | | 1.3(2) | |
| 120.6 | | 0.6(1) | |
| 141.0 | | | 5(1) |
| 171.8 | 30(3) | 25(2) | |
| 196.8 | | 2.9(4) | |
| 345.6 | 22(2) | | |
| 260.7 | | | 1000(30) |
| 401.8 | | | 11(1) |
| 461.5 | 14(2) | 13(1) | |
| 497.0 | | 2.3(3) | |
| 561.8 | | 2(1) | |
| 564.1 | 7(2) | 5(1) | |
| 685.7 | | | 15(2) |
| 682.3 | 2(1) | 2.3(3) | |
| 740.2 | 25(2) | | |
| 761.7 | 3(1) | 2.3(3) | |
| 788.0 | | 2.6(4) | |
| 826.8 | | | 975(30) |
| 969.1 | 50(4) | 50(3) | |
| 1085.8 | 47(3) | | |
| 1145.3 | 4(1) | 3.1(3) | |
| 1246.3 | | 1.3(2) | |

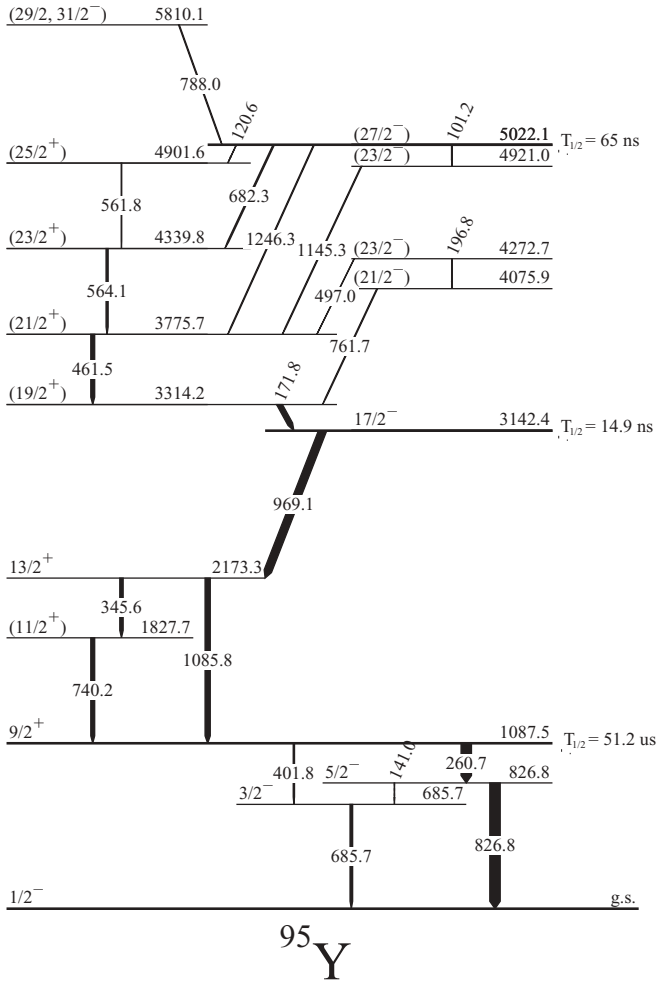


FIG. 4. Partial level scheme of $^{95}$Y, as obtained in the present work.

of the 682-keV line, which is barely visible in our data. Also the 171.8-keV line is in our spectrum stronger than the 461.5-keV line. The reason is that in our data we also see prompt side feeding to this cascade, whereas in the isomeric cascade of Ref. [15] the whole intensity measured was flowing from the isomeric level. Using the present data we corrected the order of transitions in the cascade, as presented in Fig. 4. (Figure 4 shows the complete level scheme, as obtained in this work, using also the data described in the next two sections.)

In our spectra we also see the 345.6-, 740.2-, and 1145.3-keV lines reported in Ref. [15] (with slightly different energies) and a new line at 761.7 keV and place them in the level scheme as shown in Fig. 4. In $^{248}$Cm fission data we do not see the 100-keV line reported in Ref. [15], probably because of too low a population of the high-spin isomer. The heavy-ion-induced fission used in Ref. [15], which is known to populate higher spins than those populated in spontaneous fission of $^{248}$Cm, could provide higher population of this isomer.

We have determined angular correlations between strong $\gamma$ transitions in $^{95}$Y, using techniques described in Refs. [30,31]. Angular correlations between the 171.8-, 969.1-, and 1085.8-keV transitons are shown in Fig. 5 with calculations for stretched quadrupole-quadrupole (QQ)

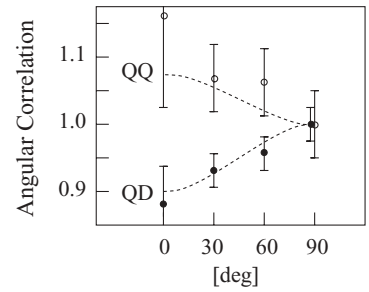


FIG. 5. Angular correlations for the 969.1- to 1085.8-keV (open circles) and 171.8- to 969.1-keV (full dots) cascades.

and quadrupole-dipole (QD) solutions. The correlation is consistent with the 969.1- and 1085.8-keV transitions being stretched quadrupole ($\Delta I = 2$) in character and the 171.8-keV transition being a stretched dipole ($\Delta I = 1$).

We have also examined $\gamma$ spectra corresponding to delayed $\gamma$ coincidences. In our measurement triple-$\gamma$ coincidences were collected within a time window of about 300 ns. The high-spin isomer reported in Ref. [15], which is now at 5022.1 keV, is populated very weakly. In contrast the 3142.4-keV level receives much higher population owing to prompt side feeding. This allowed us to find that the 3142.4-keV level is also an isomer. In Fig. 1(b) we show a spectrum doubly gated on the 171.8- and the 461.5-keV lines, where the gated lines were observed within a "prompt" time window; the spectrum displayed in Fig. 1(b) was measured within a "delayed" time window of 80–300 ns. In the spectrum one sees the 345.6-, 740.2-, 969.1-, and 1085.8-keV lines, depopulating the 3142.4-keV level.

In Fig. 6 we show a time-delayed spectrum gated on the 969.1-keV line. In the spectrum one observes a clear exponential decay (the "prompt" peak resulting from a contaminating

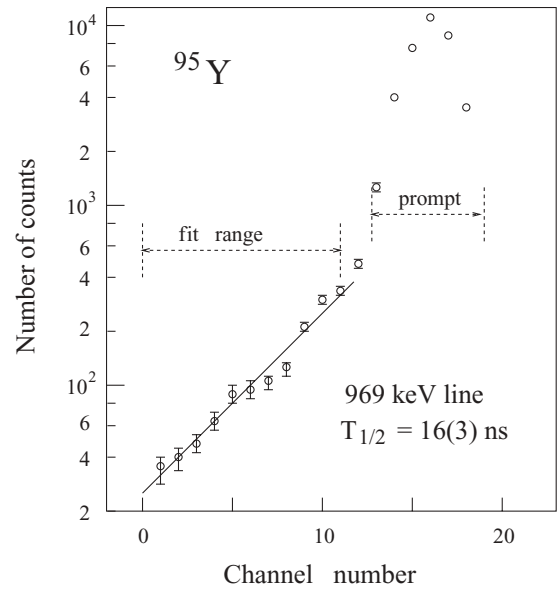


FIG. 6. Time spectrum gated on the 969.1-keV line from $^{95}$Y populated in spontaneous fission of $^{248}$Cm, as observed in the present work. The time scale is 5.5 ns/channel.

prompt contribution in the 969-keV gate). We find that the half-life of the 3142.4-keV level deduced from this spectrum, using the analysis techniques and time calibration described in Ref. [30], is $T_{1/2} = 16(3)$ ns.

Considering the energy of the 969.1-keV isomeric transition we propose that this transition has an $M2$ multipolarity. We note that the 260.6-keV transition depopulating the 1087.5-keV isomer was interpreted as an $M2$, single-particle transition between $\pi g_{9/2}$ and $\pi f_{5/2}$ orbitals [12]. It is also likely that the 682-keV isomeric transition has an $M2$ multipolarity, given the half-life of the 5022.1-keV isomer and the energy of the 682-keV isomeric transition.

These observations, the angular correlation data, and the assumption that spin is growing with excitation energy, as commonly observed in a fission process, which predominantly populates yrast states in fission fragments, allow spins to be proposed for excited levels observed in the fission of $^{248}$Cm. The stretched-quadrupole character of the 1085.8- and 969.1-keV transitions indicates spins of 13/2 and 17/2 for the 2173.3- and 3142.4-keV levels, respectively. The prompt character of the 1085.8-keV transition suggests positive parity for the 2173.3-keV level. Consequently, the proposed $M2$ character of the 969.1-keV transition points to the negative parity of the 3142.4-keV isomer. The $\Delta I = 1$ character of the 171.8-keV transition indicates spin 19/2 for the 3314.2-keV level. Further spin-parity assignments are discussed in the next section.

### B. Measurement of prompt $\gamma$ rays following spontaneous fission of $^{252}$Cf

The results from the measurement of $^{248}$Cm just presented were verified and extended in our measurement of $\gamma$ rays following the spontaneous fission of $^{252}$Cf, performed using the GAMMASPHERE ACS array at Argonne National Laboratory (see also Ref. [32] for more information on the experiment). This new measurement has some clear advantages over the $^{248}$Cm measurement, such as six times more triple-$\gamma$ coincidence events collected, three times wider time gate in the electronic setup, and a better resolution in time spectra. We needed, though, to analyze the $^{248}$Cm data first to identify excitations in $^{95}$Y. This could not be done using the $^{252}$Cf because the most abundant fission-fragment partners to $^{95}$Y produced in fission of $^{252}$Cf, which are the $^{152,153,154}$Pr nuclei, are not known sufficiently well.

From the $^{252}$Cf fission measurement we obtained $1.2 \times 10^{11}$ triple coincidences. The electronic time windows defining the coincidence events allowed measuring times in a range of 900 ns, counted from the "start" given by the "Master Gate" signal. The data were sorted into three-dimensional (3D) histograms under various conditions set on time signals, as discussed in the following.

We confirm the presence of all $\gamma$ coincidences observed in the $^{248}$Cm measurement and add new transitions to the scheme based on the $^{248}$Cm data. Figure 7(a) shows a spectrum double gated on the 969- and 172-keV lines in a 3D histogram, sorted without any time conditions (ggg cube). Apart from $\gamma$ lines seen in Fig. 1, in the $^{248}$Cm data, which are now much

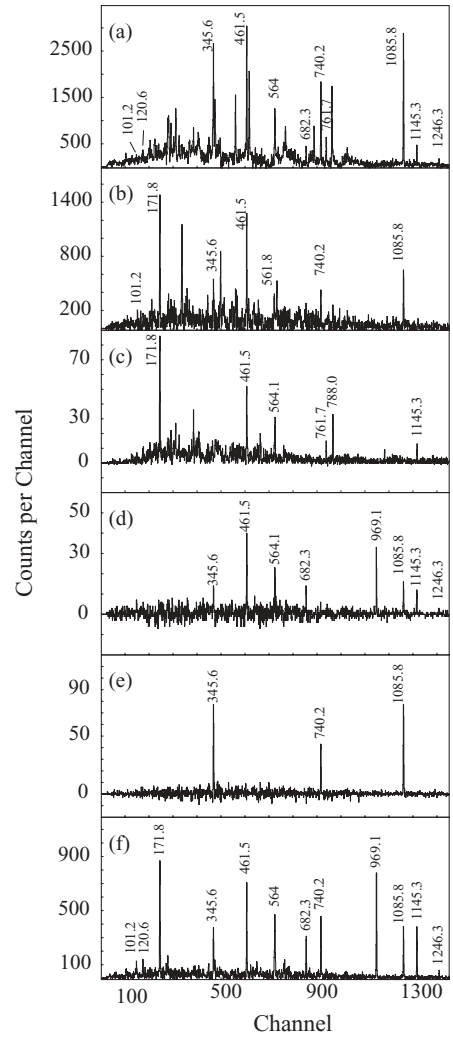


FIG. 7. Coincidence spectra gated on $\gamma$ lines in $^{95}$Y, as observed in fission of $^{252}$Cf. Energies of transitions and gates are labeled in keV. See text for more details about gated cubes.

stronger, we observe lines at 101.2, 120.6, 196.8, 497.0, 788.0, 1145.3, and 1246.3 keV. The 682.3-keV line is now clearly seen and the 564-keV line appears as a doublet with 561.8- and 564.1-keV components. This is illustrated in Fig. 7(b), which shows a spectrum double gated on the 969- and 564-keV lines. Further gating on the ggg cube allowed the placement of the newly observed transitions, as shown in the scheme in Fig. 4. The 5022.1-keV isomer is now de-excited by four transitions: 101.2, 120.6, 682.3, and 1246.3 keV. Relative $\gamma$ intensities of lines observed following fission of $^{252}$Cf are shown in the third column of Table I.

Good timing of the $^{252}$Cf data allowed sorting of 3D $\gamma$-coincidence histograms with specific conditions on time signals associated with $\gamma$ signals. These data could be used to illustrate the presence of the two isomers at 3142.4 and 5022.1 keV in $^{95}$Y. The so-called ddp cube contains triple-$\gamma$ coincidences, where along the p axis we sorted prompt $\gamma$ rays registered within the period from $-10$ to $+10$ ns relative to the "0" time given by the Master-Gate signal, and on the d axes

we sorted two $\gamma$ rays registered within the period from 40 to 210 ns after the "0" time.

Figure 7(c) shows a spectrum double gated on the 969- and 1086-keV lines on the two d axes of the ddp cube. The resulting gated spectrum contains prompt $\gamma$ decays from levels above the 3142.4-keV isomer. In the spectrum one sees the 171.8-, 461.5-, 564.1-, 761.7-, and 1145.3-keV lines. Their intensities represent the *prompt* side feeding of the levels they de-excite. Note that in this spectrum the 101.2-, 120.6-, 682.3-, and 1246.3-keV lines, depopulating the 5022.1-keV isomer, are not seen but the 788.0-keV line placed above the 5022.1-keV isomer is observed. The 788.0-keV transition depopulates the 5810.1-keV level, which is not isomeric. In the spectrum there are also other prompt lines, marked by asterisks, which we assigned to new prompt $\gamma$ transitions in the complementary Pr isotopes [33].

In Fig. 7(d) a spectrum obtained from the ddp cube is shown, where the first gate was set on the 788-keV line on the p axis and the second gate on the 172-keV line on the d axis. In the spectrum one observes delayed $\gamma$ transitions, sorted along the other d axis. These are all the transitions depopulating cascades starting from the 5022.1-keV isomer.

In Fig. 7(e) we show a spectrum obtained from the ddp cube with the first gate on the 172-keV line on the p axis and the second gate on the 969-keV line on the d axis. In the spectrum one observes delayed $\gamma$ transitions below the 3142.4-keV isomer, only.

The spectra in Figs. 7(c), 7(d), and 7(e) indicate that both the 3142.4- and the 5022.1-keV levels are isomeric. Finally, in Fig. 7(f) we show a sum of several spectra double gated on various pairs of transitions de-exciting both isomers. The gates were set in the ddd cube, sorted with the 40- to 210-ns time window on all three axes. In the spectrum one can clearly see lines corresponding to all transitions below the 5022.1-keV isomer. We note, however, that there is no 788.0-keV line, as expected.

In Figs. 8 and 9 we show time-delayed spectra for the 969.1-keV transition from the 3142.4-keV isomer and for the sum of 682.3- and 1146.3-keV transitions from the 5022.1-keV isomer in $^{95}$Y, respectively. The spectra were obtained from the pgt cube prepared in a following way: $\gamma$ signals registered within the "prompt" time window were set along the p axis, $\gamma$ signals with no time window on them were set along the g axis, and time values corresponding the g-axis $\gamma$ signals were set along the t axis (with the t range being from $-50$ to $+900$ ns relative to the "0" time). The time-delayed spectrum for the 3142.4-keV isomer was obtained by gating the 172-keV line on the p axis and the 969-keV line on the g axis. The time-delayed spectrum for the 5022.1-keV isomer was obtained by gating on the 788-keV line on the p axis and on the 682- and 1146-keV lines on the g axis. The spectra shown in Figs. 8 and 9 were binned to 2.2 and 8.8 ns/channel, respectively. It can be seen that the yield of the 3142.4-keV isomer is about an order of magnitude larger that the yield of the 5022.1-keV isomer, in accord with $\gamma$ intensities listed in Table I.

Fitting an exponential function plus constant background to the spectra in Figs. 8 and 9 gives half-lives of 14.7(5) and 62(4) ns for the 3142.4- and the 5022.1-keV isomers, respectively. The half-life of the 3142.4-keV isomer is consistent with the one obtained from $^{248}$Cm fission data. However, the half-life of the 5022.1-keV isomer found in this work is significantly shorter than the 165(42)-ns value reported in Ref. [15], though we note that the uncertainty reported in Ref. [15] is rather large. To verify our result obtained from fitting the time-delayed spectrum, we used another technique, proposed in Ref. [34], where a half-life is determined by observing intensity of triple-$\gamma$ coincidences in an isomeric cascades in cubes sorted with various time windows. The advantage of this method is the cleanness of the observed triple-$\gamma$-coincidence signal, collected over a wide time window and concentrated in a small volume in the ddd cube. Consequently, it is easier to discriminate such a signal against background than a time-delayed spectrum and

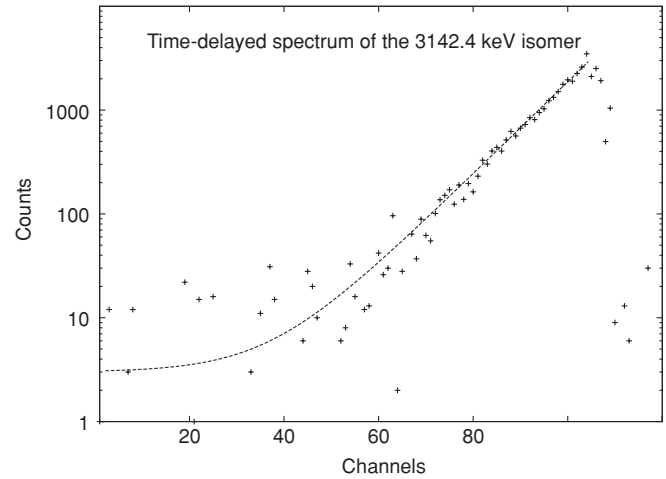


FIG. 8. Time-delayed spectrum corresponding to the decay of the 3143.4-keV isomer in $^{95}$Y populated in spontaneous fission of $^{252}$Cf, as observed in the present work. The time scale is 2.2 ns/channel. The dashed line is an exponential fit to the data, including constant background.

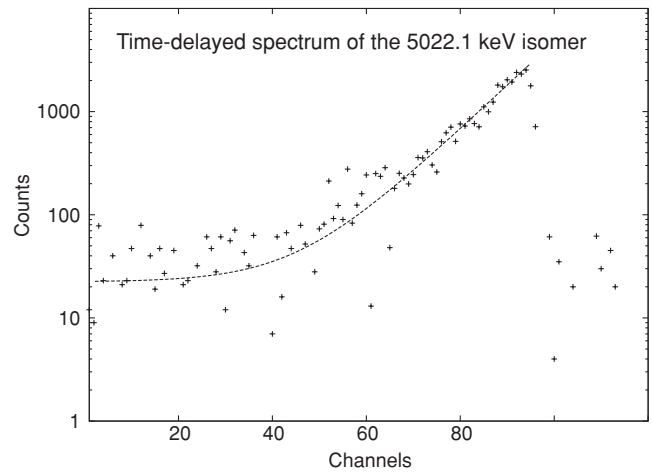


FIG. 9. Time-delayed spectrum corresponding to the decay of the 5022.1-keV isomer in $^{95}$Y, populated in spontaneous fission of $^{252}$Cf as observed in the present work. The time scale is 8.8 ns/channel. The dashed line is an exponential fit to the data, including constant background.

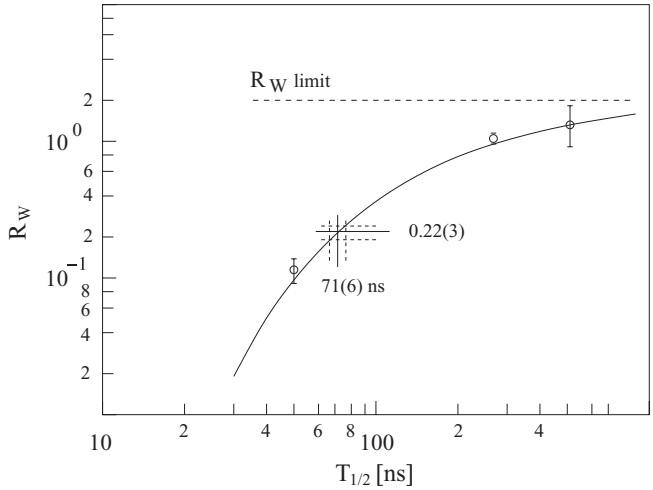


FIG. 10. Ratio $R_W$ of intensities of the isomeric cascade depopulating the 5022.1-keV isomer in $^{95}$Y, as observed in fission data of $^{252}$Cf sorted within various time windows. See text for more details.

to ensure, thanks to the triple-coincidence condition, that the signal is not contaminated by other effects.

In our work we compared the intensity of the 171.8–461.5–1145.6 keV triple-$\gamma$ cascade observed in two different ddd cubes sorted with time windows (i) from 40 to 210 ns and (ii) from 210 to 550 ns. The ratio $R$ of the two intensities depends on the half-life of the isomer depopulated by the cascade. One can easily calculate this ratio by taking integrals of exponential decay over the two time windows. Calculated values are shown in Fig. 10 as a thick line (with a log-log scale being used to allow a wide range of half-lives to be inspected). The dashed line shows the upper limit for this ratio (equal to the ratio of the widths of the two windows). In Fig. 10 we show experimental data for three known isomers, the $T_{1/2} = 52$ ns isomer in $^{130}$Sn (89–774–1221 keV triple-$\gamma$ cascade), the $T_{1/2} = 164$ ns isomer in $^{134}$Te (115–297–1279 keV triple-$\gamma$ cascade), and the $T_{1/2} = 510$ ns isomer in $^{135}$Te (89–774–1221 keV triple-$\gamma$ cascade). The agreement of the calculated curve with the data is very satisfactory, which justifies the use of this curve as a calibration, when determining half-lives of unknown isomers. The ratio $R = 0.22(3)$, obtained for the 171.8–461.5–1145.6 keV cascade, depopulating the 5022.1-keV isomer in $^{95}$Y, compared in Fig. 10 against the calibration curve, determines the half-life of the isomer to be $T_{1/2} = 71(6)$ ns, which is consistent with the value obtained before from fitting the time-delayed spectrum. We adopt a weighted average for the two values of $T_{1/2} = 65(4)$ ns as the half-life for the 5022.1-keV isomer in $^{95}$Y.

### C. Measurement of delayed $\gamma$ rays following neutron-induced fission of $^{235}$U

The excitations in $^{95}$Y discussed in the preceding two sections are located above the $9/2^+$, 1087.5-keV isomer. Because of its long half-life no $\gamma$ coincidences across this isomer could be observed in our $^{248}$Cm or $^{252}$Cf data. Searching for possible new branchings from this isomer, as well as for other long-lived states in $^{95}$Y, we performed a measurement at the LOHENGRIN fission-fragment separator [35] at ILL Grenoble. There we measured $\gamma$ rays from mass $A = 95$ ions, arriving to the detection point about 2 $\mu$s after being produced in fission of $^{235}$U induced by thermal neutrons inside the ILL reactor. In the measurement about $1.2 \times 10^8$ ions were collected.

The detection setup consisted of an ion chamber and three Ge detectors, two CLOVER detectors of 150% relative efficiency each and a 60% GammaX detector. In the measurement we used an electrostatic deflection system, developed recently at LOHENGRIN, operating at the frequency of 100 Hz chosen to search for isomers in the millisecond range. Digital electronics with a 40-MHz clock made it possible to measure half-lives in the microsecond range. For more details about the this setup see Ref. [36].

To illustrate the sensitivity of our measurement we show in Fig. 11 the time-delayed spectrum for the known 195.5-keV isomer in $^{95}$Kr, as obtained in our measurement. The half-life of 1.5(1) $\mu$s, extracted from this spectrum, is in good agreement with the previously reported value of $T_{1/2} = 1.4(2)$ $\mu$s [37]. It should be noted that $^{95}$Kr is produced at a very low rate of $7 \otimes 10^{-5}$ per $^{235}\mathrm{U} + n_{\mathrm{th}}$ fission event and the population of the 195.5-keV isomer represents a fraction of this rate only.

We searched for new isomers in the mass $A = 95$ chain using a 2D histogram (called the "gt" matrix), where on the g axis we sorted a $\gamma$ energy signal and on the t axis the registration time of this $\gamma$, measured relative to the "start" of the electrostatic deflector. Within the deflector cycle of 10 ms, mass $A = 95$ ions were collected at the detection point for the period from 0 to 5 ms (ion beam ON) and for the remaining 5 ms the ion beam was deflected (ion beam OFF). In Fig. 12(a) we show a total projection of the gt matrix on the g axis. The spectrum is dominated by background and

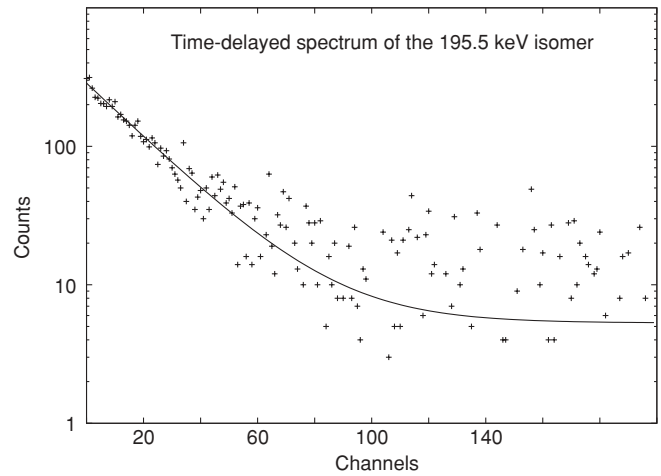


FIG. 11. Time-delayed spectrum for the 113.8-keV transition corresponding to the decay of the 195.5-keV isomer in $^{95}$Kr, as observed in fission of $^{235}\mathrm{U} + n_{\mathrm{th}}$ in this work. The time scale is 100 ns/channel. The dashed line represents an exponential fit to the data, including constant background. It may seem that the background level is fitted too low but we note that this is a spectrum with subtracted background. Therefore there are channels with zero or negative counts, which could not be plotted on a log scale.

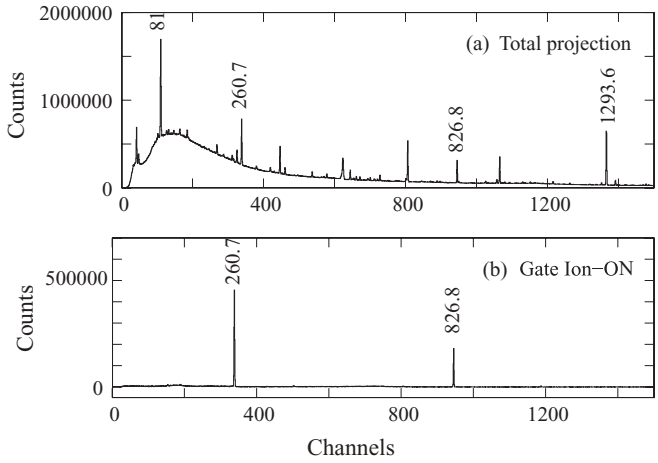


FIG. 12. (a) Total projections of the gt matrix. (b) $\gamma$ spectrum gated on the t axis of the gt matrix in the range from 0 to 5 ms, as obtained in this work. Energies of $\gamma$ lines are labeled in keV. See text for further explanation.

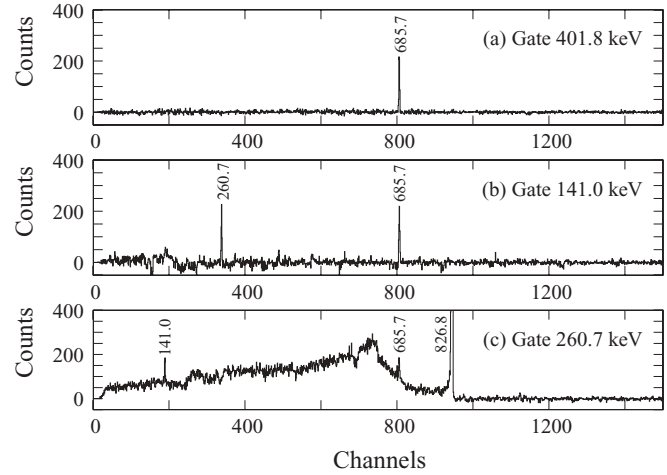


FIG. 13. Coincidence $\gamma$ spectra gated on $\gamma$ lines in $^{95}$Y, as obtained in this work from the gg matrix. The full scale in Fig. 13(c) is 25,000. Energies of transitions are labeled in keV. See text for further explanation.

$\beta$-decay lines (e.g., 1293.6 keV of $^{41}$Ar) but one can also clearly see in the spectrum the 260.7- and 826.8-keV lines corresponding to the decay of the $9/2^+$ isomer in $^{95}$Y. In Fig. 12(b) we show a background-subtracted spectrum gated on the t axis of the gt matrix in the range from 0 to 5 ms and with background selected from 9 to 10 ms (with the background being normalized to match the width of the gate). In the spectrum one observes lines corresponding to isomeric decays, only. None of the background lines seen in Fig. 12(a) are present here. Apart from the 260.7- and 826.8-keV lines there are the 81.7- and 113.8 keV lines from the decay of the 1.5-$\mu$s isomer in $^{95}$Kr, the 1087.5-keV sum peak of the 260.7- and 826.8-keV lines, and three other lines at 141.0, 401.8, and 685.7 keV, though, because of their low intensities, these lines are not visible at this large scale.

To learn about the new lines we analyzed a 2D $\gamma$-$\gamma$ histogram (gg matrix) where we sorted $\gamma$ coincidences collected during the "ion-beam-ON" period. The $\gamma$-coincidence time window was 600 ns. In Fig. 13(a) we show a spectrum gated on the 401.8-keV line, in which a 685.7-keV line is seen. The gate set on the 141.0-keV line, displayed in Fig. 13(b), shows two lines at 260.7 and 685.7 keV. Finally, the spectrum gated on the 260.7-keV line, displayed in Fig. 13(c), shows the 826.8-, 141.0-, and 685.7-keV lines. These three spectra indicate that there is a new, 401.8-keV decay branch from the $9/2^+$, 1087.5-keV isomer to the known [38] $3/2^-$, 685.7-keV level in $^{95}$Y. The 401.8-keV transition is, therefore, of pure $E3$ multipolarity. The 141.0-keV transition, which de-excites the 826.8-keV level to the 685.7-keV level, should have $M1 + E2$ multipolarity. Gamma intensities of transitions below the $9/2^+$, 1087.5-keV isomer in $^{95}$Y, as found in the spectrum shown in Fig. 12(b), are presented in column 4 of Table I.

We measured the half-life of the $9/2^+$ isomer in $^{95}$Y, using the present data. In Fig. 14(a) a time-delayed spectrum is shown, obtained from the gt-ion matrix by gating on the 260.7-keV isomeric transition. In the gt-ion matrix we sorted $\gamma$ energy (g axis) versus its time, counted from the arrival of the preceding ion. We note that it was not possible in our measurement to select ions corresponding to the 260.7-keV isomer, only. Therefore sorted into the gt-ion matrix were all ions corresponding to mass $A = 95$. A spectrum gated on background in the gt-ion matrix, normalized to the 260.7-keV gate width, was subtracted from the 260.7-keV gate. It is important to make a proper background subtraction here because in a time window of 240 $\mu$s with the ion-beam rate of about 3000 ions/s, the background is no longer flat. This is shown in Fig. 15, which displays a background- gated spectrum obtained from the gt-ion matrix. The spectrum has an exponential time dependence, which is expected when both the start (ion) and stop ($\gamma$) signals are randomly distributed in time.

The exponential fit to the spectrum in Fig. 14 gated on the 260.7-keV isomeric transition provides a half-life of $T_{1/2} = 44.0(3)$ $\mu$s. However, the fitted value, which is clearly shorter

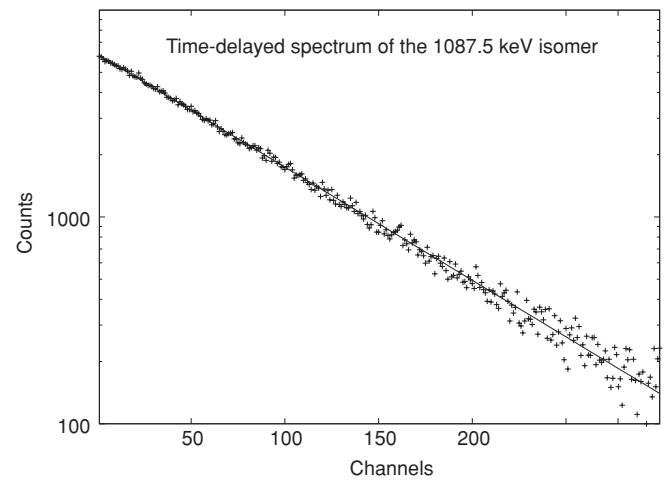


FIG. 14. Time-delayed spectrum gated on the 260.7-keV line from $^{95}$Y, as observed in the present work. In the time spectrum one channel corresponds to 0.8 $\mu$s.

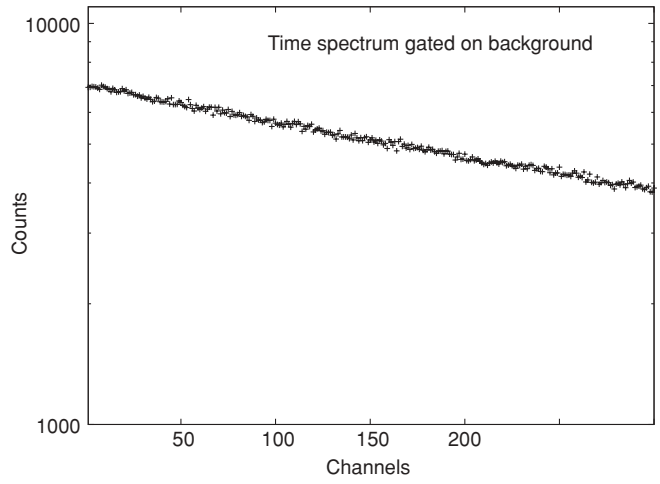


FIG. 15. Time spectrum gated on background, as observed in the present work.

than the literature half-life of 56.2(1.5) $\mu$s [38] needs further correction owing to the long half-life of the isomer. At a rate of 2600 ions/s, as measured in our experiment, the probability that another ion is observed before the ion corresponding to the 56-$\mu$s isomer decays, is no longer negligible. To check this we simulated time-delayed spectra for various combinations of half-lives and ion-beam intensities and fitted their half-lives. The results are shown in Fig. 16 for three half-lives at three beam intensities. (We checked that the results do not depend on the fraction of the "isomeric" ions in the ion beam.) The $F_{\rm cor}$ factor shown in Fig. 16 represents the ratio of the observed half-life to its true value. For instance, the 100-$\mu$s half-life measured at beam intensity of 10,000 ion/s will show up as a 41-$\mu$s half-life ($F_{\rm cor} = 0.41$). Using these simulations we found an $F_{\rm cor}$ factor of 0.860(15) for the 1087.5-keV isomer in $^{95}$Y, which gives the corrected half-life of $T_{1/2} = 51.2(9)$ $\mu$s.

Using the gt matrix we performed scans for the millisecond isomers in mass $A = 95$ isobars $^{95}$Kr, $^{95}$Rb, $^{95}$Sr, $^{95}$Y, and $^{95}$Zr, produced in the fission of $^{235}$U with measurable rates. The

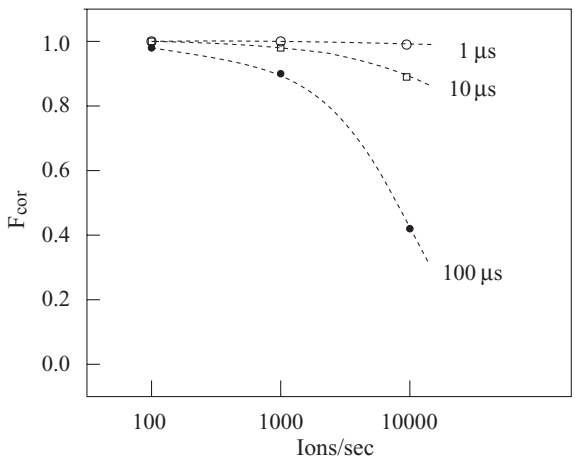


FIG. 16. Corrections to long half-lives measured at various ion-beam intensities. The dashed lines are drawn to guide the eye. See text for further explanation.

predicted production rates for these isobars are $7 \times 10^{-5}$, $8 \times 10^{-3}$, $5 \times 10^{-2}$, $1 \times 10^{-2}$, and $1 \times 10^{-3}$ per one $^{235}{\rm U} + n_{\rm th}$ fission, respectively [39]. No millisecond isomers were found in our data. Upper limits for the population of such isomers in the discussed mass $A = 95$ isobars could be estimated based on the population and the decay rate of the $9/2^+$ isomer in $^{95}$Y. The limit for observing a $\gamma$ line in our measurement was about 0.007 of $\gamma$ intensity of the 260.7-keV isomeric transition (a limit that was found to be rather independent of $\gamma$ energy). We made a conservative assumption that the population of the $9/2^+$ isomer in $^{95}$Y amounts to 100% of the total production of $^{95}$Y (i.e., $1 \times 10^{-2}$ per one fission). Then the limit for observing an isomeric state is $7 \times 10^{-5}$ relative to the total population of $^{95}$Y. Consequently, one can state that the population of millisecond isomers, relative to the total population in $^{235}{\rm U} + n_{\rm th}$ fission, is below the levels of 0.1 in $^{95}$Rb, 0.0014 in $^{95}$Sr, 0.007 in $^{95}$Y, and 0.07 in $^{95}$Zr.

### D. Rates of isomeric transitions in $^{95}$Y and octupole coupling around $N = 56$

Using the half-lives of the three isomers observed in $^{95}$Y and $\gamma$ intensities of their decay branches, as found in this work, and assuming multipolarities for these branchings as shown in Fig. 4, we estimated $\gamma$ transition rates for isomeric branches, taking into account the internal conversion process. The results are shown in Table II in units of inverse seconds and in Weisskopf units.

The observed $\gamma$ rates are consistent with expectations for single-particle transitions rates in a spherical nucleus. The $E2$ transition rate is of the order of one Weisskopf unit, similar to what is observed in the neigboring $^{96}$Zr core. The two $E3$ transitions in $^{95}$Y also do not show any significant enhancement, indicating the lack of octupole collectivity in this nucleus. This, however, is in sharp contrast to the $^{96}$Zr core, where the $E3$ decay from the $3^-$, 1897.2-keV state is reported with a very large rate of 57(4) W.u. [40]. This difference can be understood if one assumes that the $3^-$ state in the $^{96}$Zr core is an octupole vibration dominated by coupling of $g_{9/2}$ and $p_{3/2}$ *proton* orbitals, which are here close to the Fermi level. Such a vibrational coupling between protons is "blocked" in an odd-$Z$ nucleus. Therefore in $^{95}$Y one observes lower rates for $E3$ decays.

It is known that $E1$ rates are enhanced in nuclei with octupole collectivity present [41]. In $^{96}$Zr the $E1$ decay rate from the $3^-$, 1897.2-keV state is $1.23(1) \times 10^{-3}$ W.u. [40], which is about three orders of magnitude faster than an average $E1$ rate in nuclei. In contrast, the $E1$ decay rate in $^{95}$Y is more than three orders of magnitude slower than the $B(E1)$ reported in its neighbor $^{96}$Zr. The likely explanation of this difference is again the presence of octupole collectivity in $^{96}$Zr and its absence in $^{95}$Y.

These observations allow more general comments on octupole correlations around $^{96}$Zr. The fastest $E1$ transitions and the lowest energies of $3^-_1$ states are observed in the actinide and lanthanide nuclei around neutron and proton numbers $(N, Z) = (134, 88)$ and $(N, Z) = (88, 56)$, where an octupole deformation or strong octupole correlations were

TABLE II. Gamma rates of isomeric transitions in $^{95}$Y, as observed in the present work.

| $E_\gamma$ (keV) | Multipolarity | Total conversion coefficient | Gamma rate ($s^{-1}$) | Gamma rate (W.u.) |
|---|---|---|---|---|
| 101.2 | $E2$ | 1.02 | $2.9(3) \times 10^6$ | 0.85(9) |
| 120.6 | $E1$ | 0.062 | $1.4(2) \times 10^6$ | $3.8(6) \times 10^{-7}$ |
| 682.3 | $M2$ | 0.0039 | $5.2(6) \times 10^6$ | 0.077(9) |
| 1246.3 | $E3$ | 0.00074 | $2.9(4) \times 10^6$ | 2.0(3) |
| 969.1 | $M2$ | 0.0016 | $6.7(3) \times 10^7$ | 0.17(1) |
| 260.7 | $M2$ | 0.0693 | $1.81(4) \times 10^4$ | 0.033(1) |
| 401.8 | $E3$ | 0.0256 | $2.0(2) \times 10^2$ | 2.7(3) |

reported [42–45]. At these proton or neutron numbers, pairs of orbitals with $\Delta j = \Delta l = 3$ ($\Delta 3$ orbits) are close in energy, allowing an enhanced octupole coupling. In the two regions both protons and neutrons contribute to octupole coupling and strong octupole effects are observed in both odd-$N$ [46,47] and odd-$Z$ [48,49] nuclei as well as in odd-odd nuclei [50,51]. It is important to note that in the two regions the octupole coupling is helped by the quadrupole deformation via the spin-orbit interaction, which brings closer subshells of the $\Delta 3$ orbits. For example, the $\Omega = 1/2$ subshell of the $\pi h_{11/2}$ and $\pi d_{5/2}$ (i.e., the 1/2[550] and the 1/2[420] Nilsson orbitals) are only 0.5 MeV apart already at a rather low deformation of $\beta_2 = 0.17$ [52]. They can be mixed by octupole interaction much easier than the spherical $\pi h_{11/2}$ and $\pi d_{5/2}$ orbitals, which are separated by about 2.3 MeV [52]. It is also worth noting that spherical neutron $\Delta 3$ orbits are, generally, further apart than the spherical proton $\Delta 3$ orbits. In particular the $h_{11/2}$ and $d_{5/2}$ neutron orbitals are, according to our estimates [4] (see also Sec. III), about 3 MeV apart, compared to 2.3 MeV for protons. Therefore, despite residing at $N = 56$ neutrons, the spherical $^{96}$Zr and its neighbors may have weak octupole coupling between the $h_{11/2}$ and $d_{5/2}$ *neutron* orbitals. Consequently, as previously suggested, octupole collectivity in these nuclei would be primarily from the coupling of $\pi g_{9/2}$ and $\pi p_{3/2}$ orbitals. The maximum of the effect should be observed in nuclei where the $\pi p_{3/2}$ orbital is just filled. It is known that the $\pi p_{3/2}$ and $\pi f_{5/2}$ orbits are very close to each other in this region, but their order is still being disputed. Therefore, this maximum is expected somewhere between $Z = 32$ and $Z = 38$. In Ref. [53] a $3^-$ state was reported at 1506 keV in the $^{90}_{36}$Kr$_{54}$ nucleus, which is the lowest $3^-$ excitation in the region found to date, suggesting that octupole correlations may be even stronger there than in $^{96}$Zr.

The $M2$ rates observed for isomeric transitions in $^{95}$Y are consistent with a general observation that such an $M2$ rate is a fraction of a Weisskopf unit for nuclei with mass $A > 40$ (Nuclear Data Sheets recommendations) [54,55]). As proposed in Sec. III, all three discussed $M2$ transitions have dominating components corresponding to the single-particle transition between $\pi g_{9/2}$ and $\pi f_{5/2}$ orbitals. In case of the $9/2^+$, 1087.5 keV and the $27/2^-$, 5022.1-keV isomers, which contain the $g_{9/2}$ single-particle proton level in their structure, the observed $M2$ decay rates are similar. These $M2$ decays contain contribution from the $\pi g_{9/2} \rightarrow \pi f_{5/2}$ single-particle transition. The $M2$ rate from the $17/2^-$, 3142.4-keV isomer is larger. As discussed in Sec. III, this isomer may have more complex structure, involving core excitations. We note that in this case the $M2$ decay contains contribution from the $\pi f_{5/2} \rightarrow \pi g_{9/2}$ single-particle transition, where the final spin is larger than in the other two decays.

We summarize this section with a note that the observed $\gamma$ rates of isomeric transitions in $^{95}$Y support the spin assignments as proposed in Fig. 4. The explanation of octupole excitations around $^{96}$Zr requires the positions of the $\pi p_{3/2}$ and the $\nu h_{11/2}$ orbitals to be found, which provides further motivation for our searches for the key orbits in this region, as mentioned in Sec. I.

## III. SHELL-MODEL CALCULATIONS FOR $^{95}$Y

The orbitals available to form medium-spin, near-yrast excitations in $^{95}$Y are $\nu d_{5/2}$, $\nu g_{7/2}$, and $\nu h_{11/2}$ for neutrons and $\pi f_{5/2}$ and $\pi g_{9/2}$ for protons. Excited levels above the 1087.5-keV isomer are expected to involve excitations from the $^{94}$Sr core coupled to the odd proton in $^{95}$Y. The lowest excitations in $^{94}$Sr are due to a pair of neutrons, occupying the $\nu g_{7/2}$ or the $\nu d_{5/2}$ orbitals and forming multiplet of levels with spins $2^+$, $4^+$, and $6^+$. The prompt character of the 345.6-, 740.2-, and 1085.8-keV transitions suggests that the 1827.7- and 2173.3-keV levels are due to such core excitations coupled to the odd proton in the $\pi g_{9/2}$ orbital. In particular the 2173.3-keV level may correspond to the $\pi g_{9/2} \otimes (2^+)_{\rm core}$ configuration. Consequently, the structure of the $17/2^-$, 3142.4-keV isomer may involve the odd proton in the $\pi f_{5/2}$ orbital (coupled to a $6^+$ core excitation), given the $M2$ character of the 969.1-keV transition.

Looking for a possible interpretation of the 5022.1-keV isomer we note that in $^{97}$Y there is a long-lived, $27/2^-$ isomer at 3523 keV, interpreted as the $\pi g_{9/2} \otimes \nu(g_{7/2}h_{11/2})_{9^-}$ configuration. Such maximum-aligned configurations are usually yrast in character and receive appreciable population in fission. We propose that the 5022.1-keV isomer in $^{95}$Y has the same configuration. The excitation energy of this configuration in $^{95}$Y is higher than in $^{97}$Y owing to lower population of both $\nu g_{7/2}$ and $\nu h_{11/2}$ orbitals in $^{95}$Y.

One more three-particle state can be created above the $27/2^-$ isomer by promoting the neutron from the $\nu g_{7/2}$ to the $\nu h_{11/2}$ orbital, forming the $\pi g_{9/2} \otimes \nu(h_{11/2})^2$ fully aligned configuration. This could explain the 5810.1-keV excitation in

$^{95}$Y, if its spin is $29/2^+$. In case the spin of the 5810.1-keV level is $29/2^-$ or $31/2^-$, core excitations coupled to the $27/2^-$ isomer should be involved. A similar situation was encountered in $^{94}$Sr [4], where the 5740.8-keV level with spin of 10 or $11^-$ was observed 882 keV above the $\nu(g_{7/2}h_{11/2})_{9^-}$ excitation. It was proposed that this level could either be due to $[\nu(h_{11/2})^2]_{10^+}$ excitation or due to the core $\otimes\ \nu(g_{7/2}h_{11/2})_{9^-}$ coupling. However, in $^{94}$Sr another core-multiparticle coupling was also proposed, namely that of the ground-state cascade to the $\pi(g_{9/2})^2_{8^+}$ two-proton excitation [56]. In Ref. [4] we argued against this option and here is another argument. If the 5740.8-keV excitation in $^{94}$Sr and the 5810.1-keV excitation in $^{95}$Y are of the same origin, which is likely considering similarities between the two levels, then this cannot be the core $\otimes\ \pi(g_{9/2})^2_{8^+}$ configuration, which is unlikely in $^{95}$Y, as it should correspond in fact to the four-particle-core coupling in this nucleus.

Because of the proposed $M2$ multipolarity of the 682.3-keV transition the configuration of the 4339.8-keV level should involve the $\pi f_{5/2} \otimes \nu(g_{7/2}h_{11/2})_{9^-}$ configuration with spin $23/2^+$. Consequently, for the 3775.7-keV level the $[\pi p_{3/2} \otimes \nu(g_{7/2}h_{11/2})_{9^-}]_{21/2^+}$ configuration could be proposed and for the 3314.2-keV level the $[\pi p_{1/2} \otimes \nu(g_{7/2}h_{11/2})_{9^-}]_{19/2^+}$ configuration is indicated.

The discussed configurations are understood as the so-called dominating configurations, whereas the complete structure of excitations may be more complex, involving numerous small contributions from other couplings. To verify the proposed dominating configurations and to find their contributions in the key yrast excitations in $^{95}$Y, we performed shell-model calculations using a large valence space based on the $^{78}$Ni core, including $(1f_{5/2}, 2p_{1/2}, 2p_{3/2}, 1g_{9/2})$ orbitals for protons and $(2d_{5/2}, 3s_{1/2}, 2d_{3/2}, 1g_{7/2}, 1h_{11/2})$ for neutrons, dubbed hereafter $\pi(r3-g)$, $\nu(r4-h)$ space. In particular, we were interested in identifying those excitations that comprise in their structure the $\nu(g_{7/2}h_{11/2})_{9^-}$ neutron coupling.

The effective interaction used in this work was derived from the CD-Bonn nucleon-nucleon potential using $G$-matrix theory and adapted to the model space using many-body perturbation theory techniques [57]. The proton-proton part of the interaction has been discussed in Ref. [58]. The proton-neutron effective Hamiltonian was corrected in its monopole part to ensure the basic propagation of the single-particle states between $^{79}$Ni and $^{91}$Zr [$\pi(r3)$–$\nu(r4-h)$ monopoles] and between $^{91}$Zr and $^{101}$Sn [$\pi(g_{9/2})$–$\nu(r4-h)$ monopoles]. Similarly, monopole corrections were applied to the neutron-neutron interaction to reproduce the basic spectroscopy along the tin chain. The unknown centroid of $h_{11/2}$ was estimated to be around 3 MeV as in previous calculations in that region [4]. As the monopole tuning of the present interaction is a part of a broader study [10,59], no specific modifications were further applied for the case of $^{95}$Y.

The calculations were performed using the m-scheme code ANTOINE [60] in a truncated space, allowing for 8p-8h excitations with respect to the $Z=40$ and $N=56$ shell closures. For the feasibility of the calculations the occupancy of the $h_{11/2}$ orbital was further constrained to maximally four particles, which reduces substantially the sizes of diagonalized matrices (e.g., the largest size, which is that for the $1/2^-$ state, diminishes from 2,899,830,758 to 684,178,067) and has no influence on most of the levels, in which the calculated $h_{11/2}$ orbital occupancy is only fractional. We have further verified for the $29/2^+$ level that the main contributions in the wave function remain the same when the excitations to the $h_{11/2}$ orbital are not constrained. One should however keep in mind that the accuracy of the present shell-model calculations is limited (e.g., by imperfections in the effective interaction, by the uncertainty of the localization of the $\nu h_{11/2}$ orbital, and by computational resources).

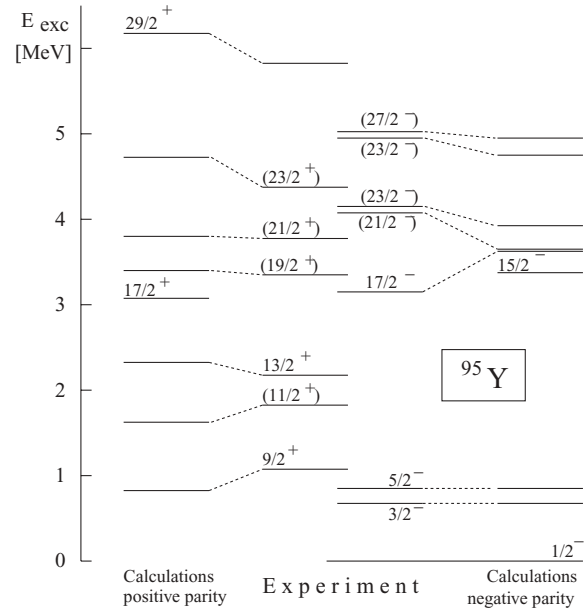


FIG. 17. Comparison of the experimental to the calculated energies of excited states in $^{95}$Y, as obtained in the present work.

The overall reproduction of the experimental spectra is, however, satisfying, as can be seen in Fig. 17. The most substantial discrepancy in our calculations concerns the $17/2^-$ state, which lies almost 500 keV too high with respect to the measurement. In this case, however, we expect that a coupling of a core-excited $3^-$ to the $11/2^+$, which is missing in the calculations, may contribute to this level. Other calculated levels can be, *a priori*, explained within the assumed model space. In particular, the $27/2^-$ isomer with the dominant $\pi g^1_{9/2} \otimes (\nu g^1_{7/2} h^1_{11/2})$ configuration is well placed in energy and supports the experimental level assignment. The calculated $29/2^+$ level, which consists mostly of the $\pi g_{9/2} \otimes (\nu h^2_{11/2})$ excitation, deviates from the experimental value by 375 keV; nonetheless, the energy of this state on the 8p-8h level is still not converged. Thus the experimental level at 5810 keV can be very likely explained as the $[\pi g_{9/2} \otimes (\nu h^2_{11/2})]_{29/2^+}$ coupling.

## IV. SUMMARY

Medium-spin excitations in the $^{95}$Y nucleus, located above the $9/2^+$ isomer, were studied experimentally and interpreted using shell-model calculations. An isomeric cascade reported as excitations in $^{96}$Y in a previous study [15] was shown to belong to $^{95}$Y from our measurement of prompt $\gamma$ rays

following fission of $^{248}$Cm, performed using EUROGAM2 ACS array. We placed this cascade on top of the $9/2^+$, 1087.5-keV isomer in $^{95}$Y. In the same measurement a new isomer at 3124.4 keV was identified, for which we determined a half-life of 14.9(5) ns. The second measurement, made in this work using the GAMMASPHERE ACS array, of $\gamma$ rays following fission of $^{252}$Cf has revealed new decay branches of the isomer reported in Ref. [15] and a prompt transition feeding this isomer. For this isomer, which we placed at 5022.1 keV and assigned spin and parity $27/2^-$, a new half-life of 65(4) ns was determined in this work. For this isomer we found new $E3$ and $E1$ decay branches.

We also searched for millisecond isomers in $^{95}$Y populated in the fission of $^{235}$U induced by thermal neutrons, using the LOHENGRIN fission-fragment separator. No millisecond isomers were observed in the mass $A = 95$ isobars $^{95}$Kr, $^{95}$Rb, $^{95}$Sr, $^{95}$Y, and $^{95}$Zr. Upper limits for the population of such isomers, relative to the total population in $^{235}\mathrm{U} + n_{\mathrm{th}}$ fission, were found to be 0.1 in $^{95}$Rb, 0.0014 in $^{95}$Sr, 0.007 in $^{95}$Y, and 0.07 in $^{95}$Zr.

For the $9/2^+$, 1087.5-keV isomer in $^{95}$Y populated in the $^{235}\mathrm{U} + n_{\mathrm{th}}$ fission we found a new $E3$ decay branch, and the half-life of this isomer, determined in the LOHENGRIN measurement, is $T_{1/2} = 51.2(9)$ $\mu$s. The $B(E3) = 2.0$ W.u. and $B(1) = 3.8 \times 10^{-7}$ W.u. transition rates in $^{95}$Y, determined in this work, are significantly lower than the analogous $B(E3) = 57$ W.u. and $B(1) = 1.23 \times 10^{-3}$ W.u. rates in the neighboring $^{96}$Zr core nucleus. This difference is interpreted as due to a much lower octupole collectivity in $^{95}$Y as compared to $^{96}$Zr. This observation suggests that octupole effects in this region are primarily due to the coupling between $\Delta j = 3$ proton orbits $\pi g_{9/2}$ and $\pi p_{3/2}$, which is blocked in the odd-$Z$ nucleus $^{95}$Y. The low level of octupole coupling between neutrons is probably due to a larger separation of the key $\Delta j = 3$, $\nu h_{11/2}$ and $\nu d_{5/2}$ orbitals as compared to the $\Delta j = 3$ proton pair. Further studies of the energies of single-particle levels in this region are required to verify the proposed explanations.

All three isomers observed in $^{95}$Y have $M2$ decay branches with similar transition rates of the order of 0.1 W.u. The nature of these decays was explained by the shell-model calculations done in this work, which reproduce fairly excitations in $^{95}$Y. Configurations of excited levels found in the calculations indicate that all three isomeric $M2$ transitions in $^{95}$Y correspond to a single-particle transition between the $f_{5/2}$ and $g_{9/2}$ proton orbitals.

## ACKNOWLEDGMENTS

The authors are indebted for the use of $^{248}$Cm to the Office of Basic Energy Sciences, US Department of Energy, through the transplutonium element production facilities at the Oak Ridge National Laboratory. This work was supported by the Polish MNiSW Grant No. N N202 007334 and by the Department of Energy, Office of Nuclear Physics, under Contract No. DE-AC02-06CH11357.

[1] T. Werner, J. Dobaczewski, M. W. Guidry, W. Nazarewicz, and J. A. Sheikh, Nucl. Phys. **A578**, 1 (1994).
[2] J. Skalski, S. Mizutori, and W. Nazarewicz, Nucl. Phys. **A617**, 282 (1997).
[3] W. Urban, J. L. Durell, A. G. Smith, W. R. Phillips, M. A. Jones, B. J. Varley, T. Rząca-Urban, I. Ahmad, L. R. Morss, M. Bentaleb, and N. Schultz, Nucl. Phys. **A689**, 605 (2001).
[4] T. Rząca-Urban, K. Sieja, W. Urban, F. Nowacki, J. L. Durell, A. G. Smith, and I. Ahmad, Phys. Rev. C **79**, 024319 (2009).
[5] W. Urban, J. A. Pinston, J. Genevey, T. Rząca-Urban, A. Złomaniec, G. Simpson, J. L. Durell, W. R. Philips, A. G. Smith, B. J. Varley, I. Ahmad, and N. Schulz, Eur. Phys. J. A **22**, 241 (2004).
[6] W. Urban, J. A. Pinston, T. Rząca-Urban, J. Genevey, A. Złomaniec, G. Simpson, J. L. Durell, W. R. Philips, A. G. Smith, B. J. Varley, I. Ahmad, and N. Schulz, Eur. Phys. J. A **16**, 11 (2003).
[7] P. Federman and S. Pittel, Phys. Lett. **B69**, 385 (1977); **B77**, 29 (1978); P. Federman, S. Pittel, and R. Campos, *ibid.* **B82**, 9 (1979); P. Federman and S. Pittel, Phys. Rev. C **20**, 820 (1979).
[8] M. A. C. Hotchkis, J. L. Durell, J. B. Fitzgerald, A. S. Mowbray, W. R. Phillips, I. Ahmad, M. Carpenter, R. V. F. Janssens, T. L. Khoo, E. F. Moore, L. R. Morss, Ph. Benet, and D. Ye, Nucl. Phys. **A530**, 111 (1991).
[9] T. Otsuka, T. Suzuki, R. Fujimoto, H. Grawe, and Y. Akaishi, Phys. Rev. Lett. **95**, 232502 (2005).
[10] K. Sieja, F. Nowacki, K. Langanke, and G. Martínez-Pinedo (submitted to Phys. Rev. C).
[11] D. Pantelica *et al.*, Phys. Rev. C **72**, 024304 (2005).
[12] B. Pfeiffer, E. Monnand, J. A. Pinston, F. Schussler, G. Jung, J. Munzel, and H. Wollnik, in *Proceedings of the International Conference Nuclei Far from Stability, Helsingor, Denmark*, Vol. 2 (1981), p. 423.
[13] M. L. Stolzenwald, G. Lhersonneau, S. Brant, G. Menzen, and K. Sistemich, Z. Phys. A **327**, 359 (1987).
[14] S. Brant, G. Lhersonneau, M. L. Stolzenwald, and K. Sistemich, Z. Phys. A **329**, 301 (1988).
[15] M. Houry, Ph.D. thesis (Université de Paris XI, 2000).
[16] R. B. Walton and R. E. Sund, Phys. Rev. **178**, 1894 (1969).
[17] W. Herzog and W. Grimm, Z. Phys. **266**, 397 (1974).
[18] R. Sellam, Ph.D. thesis (University Grenoble, 1976).
[19] E. Monnand, J. Blachot, F. Schussler, J. P. Bocquet, B. Pfeiffer, G. Sadler, H. A. Selic, T. A. Khan, W. D. Lauppe, H. Lawin, and K. Sistemich, in Int. Conf. Nuclei Far from Stability, Carges, Corsica, Abs. A26 (1976).
[20] B. Proot and J. Uyttenhove, Nucl. Instrum. Methods **192**, 447 (1982).
[21] P. J. Nolan, F. A. Beck, and D. B. Fossan, Annu. Rev. Nucl. Part. Sci. **44**, 561 (1994).
[22] W. Urban, M. A. Jones, C. J. Pearson, I. Ahmad, M. Bentaleb, J. L. Durell, M. J. Leddy, E. Lubkiewicz, L. R. Morss, W. R. Phillips, N. Schulz, A. G. Smith, and B. J. Varley, Nucl. Instrum. Methods A **365**, 596 (1995).
[23] T. Rząca-Urban, W. R. Phillips, J. L. Durell, W. Urban, B. J. Varley, C. J. Pearson, J. A. Shannon, I. Ahmad, C. J. Lister, L. R. Morss, K. L. Nash, C. W. Williams, M. Bentaleb, E. Lubkiewicz, and N. Schulz, Phys. Lett. **B348**, 336 (1995).

[24] W. Urban, J. L. Durell, W. R. Phillips, A. G. Smith, M. A. Jones, I. Ahmad, A. R. Barnet, S. J. Dorning, M. J. Leddy, E. Lubkiewicz, L. R. Morss, T. Rząca-Urban, R. A. Sareen, N. Schulz, and B. J. Varley, Z. Phys. A **358**, 145 (1997).
[25] W. Urban, T. Rząca-Urban, A. Syntfeld-Każuch, J. L. Durell, A. G. Smith, B. J. Varley, and I. Ahmad, Phys. Rev. C **76**, 037301 (2007).
[26] W. Urban, W. R. Phillips, J. L. Durell, M. A. Jones, M. Leddy, C. J. Pearson, A. G. Smith, B. J. Varley, I. Ahmad, L. R. Morss, M. Bentaleb, E. Lubkiewicz, and N. Schulz, Phys. Rev. C **54**, 945 (1996).
[27] W. Urban, W. R. Phillips, N. Schulz, B. J. P. Gall, I. Ahmad, M. Bentaleb, J. L. Durell, M. A. Jones, M. J. Leddy, E. Lubkiewicz, L. R. Morss, A. G. Smith, and B. J. Varley, Phys. Rev. C **62**, 044315 (2000).
[28] J. Kurpeta, W. Urban, Ch. Droste, A. Plochocki, S. G. Rohozinski, T. Rząca-Urban, T. Morek, L. Prochniak, K. Starosta, J. ÄystÖ, H. Penttilä, J. L. Durell, A. G. Smith, G. Lhersonneau, and I. Ahmad, Eur. Phys. J. A **33**, 307 (2007).
[29] W. Urban, T. Rząca-Urban, A. Korgul, J. L. Durell, M. J. Leddy, M. A. Jones, W. R. Phillips, A. G. Smith, B. J. Varley, I. Ahmad, L. R. Morss, and N. Schulz, Phys. Rev. C **65**, 024307 (2002).
[30] W. Urban, M. A. Jones, J. L. Durell, M. J. Leddy, W. R. Phillips, A. G. Smith, B. J. Varley, I. Ahmad, L. R. Morss, M. Bentaleb, E. Lubkiewicz, and N. Schulz, Nucl. Phys. **A613**, 107 (1997).
[31] M. A. Jones, W. Urban, and W. R. Phillips, Rev. Sci. Instrum. **69**, 4120 (1998).
[32] D. Patel, A. G. Smith, G. S. Simpson, R. M. Wall, J. F. Smith, O. J. Onakanmi, I. Ahmad, J. P. Greene, M. P. Carpenter, T. Lauritsen, C. J. Lister, R. F. Janssens, F. G. Kondev, D. Seweryniak, B. J. P. Gall, O. Dorveaux, and B. Roux, J. Phys. G: Nucl. Part. Phys. **28**, 649 (2002).
[33] W. Urban *et al.* (to be published).
[34] J. K. Hwang, A. V. Ramayya, J. H. Hamilton, D. Fong, C. J. Beyer, K. Li, P. M. Gore, E. F. Jones, Y. X. Luo, J. O. Rasmussen, S. J. Zhu, S. C. Wu, I. Y. Lee, M. A. Stoyer, J. D. Cole, G. M. Ter-Akopian, A. Daniel, and R. Donangelo, Eur. Phys. J. A **25**, 463 (2005).
[35] E. Moll *et al.*, Kerntechnik **19**, 374 (1977).
[36] A. Złomaniec, H. Faust, J. Genevey, J. A. Pinston, T. Rząca-Urban, G. S. Simpson, I. Tsekhanovich, and W. Urban, Phys. Rev. C **72**, 067302 (2005).
[37] J. Genevey, R. Guglielmini, R. Orlandi, J. A. Pinston, A. Scherillo, G. Simpson, I. Tsekhanovich, N. Warr, and J. Jolie, Phys. Rev. C **73**, 037308 (2006).
[38] T. W. Burrows, Nucl. Data Sheets **68**, 635 (1993).
[39] T. R. England and B. F. Rider, LA-UR-94-3106, ENDF-349 (1993), available at http://ie.lbl.gov/ (Fission Home Page).
[40] D. Abriola and A. A. Sonzogni, Nucl. Data Sheets **109**, 2501 (2008).
[41] G. Leander, W. Nazarewicz, G. F. Bertsch, and J. Dudek, Nucl. Phys. **A453**, 58 (1986).
[42] W. Kurcewicz, E. Ruchowska, N. Kaffrell, T. Björnstad, and G. Nyman, Nucl. Phys. **A356**, 15 (1981).
[43] W. R. Phillips, I. Ahmad, H. Emling, R. Holzmann, R. V. F. Janssens, T.-L. Khoo, and M. W. Drigert, Phys. Rev. Lett. **57**, 3257 (1986).
[44] W. Urban, R. M. Lieder, W. Gast, G. Hebbinghaus, A. Kramer-Flecken, K. P. Blume, and H. Hübel, Phys. Lett. **B185**, 331 (1987).
[45] N. Schulz, V. Vanin, M. Aïche, A. Chevallier, J. Chevallier, J. C. Sens, Ch. Briançon, S. Ćwiok, E. Ruchowska, J. Fernandez-Niello, Ch. Mittag, and J. Dudek, Phys. Rev. Lett. **63**, 2645 (1989).
[46] M. Wieland, J. Fernandez-Niello, F. Riess, M. Aïche, A. Chevallier, J. Chevallier, N. Schulz, J. C. Sens, Ch. Briançon, R. Kulessa, and E. Ruchowska, Phys. Rev. C **45**, 1035 (1992).
[47] M. A. Jones, W. Urban, J. L. Durell, M. J. Leddy, W. R. Phillips, A. G. Smith, B. J. Varley, I. Ahmad, L. R. Morss, M. Bentaleb, E. Lubkiewicz, and N. Schulz, Nucl. Phys. **A605**, 133 (1996).
[48] W. Urban, J. C. Bacelar, W. Gast, G. Hebbinghaus, A. Kramer-Flecken, R. M. Lieder, T. Morek, and T. Rząca-Urban, Phys. Lett. **B247**, 238 (1990).
[49] M. Aïche, M. Bentaleb, Ch. Briançon, A. Chevallier, J. Chevallier, J. S. Dionisio, J. Fernandez-Niello, R. Kulessa, E. Lubkiewicz, C. Mittag, F. Riess, E. Ruchowska, N. Schulz, A. Serghour, J. C. Sens, Ch. Vieu, and W. Wieland, Nucl. Phys. **A567**, 685 (1994).
[50] N. Schulz, V. Vanin, M. Aïche, Ch. Briançon, A. Chevallier, J. Chevallier, M. E. Debray, A. J. Kreiner, E. Ruchowska, and J. C. Sens, Z. Phys. A **335**, 107 (1990).
[51] J. R. Jongman, J. C. S. Bacelar, W. Urban, R. F. Noorman, J. van Pol, Th. Steenbergen, M. J. A. de Voigt, J. Nyberg, G. Sletten, J. S. Dionisio, and Ch. Vieu, Phys. Rev. C **50**, 3159 (1994).
[52] G. Leander, W. Nazarewicz, P. Olanders, I. Ragnarsson, and J. Dudek, Phys. Lett. **B152**, 284 (1985).
[53] T. Rząca-Urban, W. Urban, A. Kaczor, J. L. Durell, M. J. Leddy, M. A. Jones, W. R. Phillips, A. G. Smith, B. J. Varley, I. Ahmad, L. R. Morss, M. Bentaleb, E. Lubkiewicz, and N. Schulz, Eur. Phys. J. A **9**, 165 (2000).
[54] M. A. Lee, Nucl. Data Sheets **50**, 563 (1987).
[55] D. Kurath and R. D. Lawson, Phys. Rev. **161**, 915 (1967).
[56] E. A. Stefanova, M. Danchev, R. Schwengner, D. L. Balabanski, M. P. Carpenter, M. Djongolov, S. M. Fischer, D. J. Hartley, R. V. F. Janssens, W. F. Mueller, D. Nisius, W. Reviol, L. L. Riedinger, and O. Zeidan, Phys. Rev. C **65**, 034323 (2002).
[57] M. Hjorth-Jensen, T. Kuo, and E. Osnes, Phys. Rep. **261**, 125 (1995).
[58] A. F. Lisetskiy, B. A. Brown, M. Horoi, and H. Grawe, Phys. Rev. C **70**, 044314 (2004).
[59] L. Cáceres *et al.*, Phys. Rev. C (to be published).
[60] E. Caurier and F. Nowacki, Acta Phys. Pol. B **30**, 705 (1999).